Title

Model-Based Efficacy and Toxicity Comparisons of Moxifloxacin for Multidrug-Resistant Tuberculosis

Journal

Open Forum Infectious Diseases, 9(3)

ISSN

2328-8957

Authors

Yun, Hwi-Yeol
Chang, Vincent
Radtke, Kendra K
et al.

Publication Date

2022-03-01

DOI

10.1093/ofid/ofab660

Peer reviewed

Open Forum Infectious Diseases

MAJOR ARTICLE

Model-Based Efficacy and Toxicity Comparisons of Moxifloxacin for Multidrug-Resistant Tuberculosis

Hwi-Yeol Yun,[1] Vincent Chang,[2] Kendra K. Radtke,[2] Qianwen Wang,[2] Natasha Strydom,[2] Min Jung Chang,[3,4,5,a] and Radojka M.Savic[2,a]

[1]Department of Pharmacy, College of Pharmacy, Chungnam National University, Daejeon, Republic of Korea, [2]Department of Bioengineering and Therapeutic Sciences, University of California San Francisco, San Francisco, California, USA, [3]Department of Pharmacy and Yonsei Institute of Pharmaceutical Sciences, Yonsei University, Incheon, Republic of Korea, [4]Department of Pharmaceutical Medicine and Regulatory Science, Yonsei University, Incheon, Republic of Korea, and [5]Graduate Program of Industrial Pharmaceutical Science, Yonsei University, Incheon, Republic of Korea

Background. Moxifloxacin (MOX) is used as a first-choice drug to treat multidrug-resistant tuberculosis (MDR-TB); however, evidence-based dosing optimization should be strengthened by integrative analysis. The primary goal of this study was to evaluate MOX efficacy and toxicity using integrative model-based approaches in MDR-TB patients.

Methods. In total, 113 MDR-TB patients from 5 different clinical trials were analyzed for the development of a population pharmacokinetics (PK) model. A final population PK model was merged with a previously developed lung-lesion distribution and QT prolongation model. Monte Carlo simulation was used to calculate the probability target attainment value based on concentration. An area under the concentration-time curve (AUC)-based target was identified as the minimum inhibitory concentration (MIC) of MOX isolated from MDR-TB patients.

Results. The presence of human immunodeficiency virus (HIV) increased clearance by 32.7% and decreased the AUC by 27.4%, compared with HIV-negative MDR-TB patients. A daily dose of 800 mg or a 400-mg, twice-daily dose of MOX is expected to be effective in MDR-TB patients with an MIC of ≤0.25 μg/mL, regardless of PK differences resulting from the presence of HIV. The effect of MOX in HIV-positive MDR-TB patients tended to be decreased dramatically from 0.5 μg/mL, in contrast to the findings in HIV-negative patients. A regimen of twice-daily doses of 400 mg should be considered safer than an 800-mg once-daily dosing regimen, because of the narrow fluctuation of concentrations.

Conclusions. Our results suggest that a 400-mg, twice-daily dose of MOX is an optimal dosing regimen for MDR-TB patients because it provides superior efficacy and safety.

Keywords. lung lesion distribution model; moxifloxacin; multidrug resistance tuberculosis (MDR-TB); population pharmacokinetics; QT prolongation model.

Tuberculosis (TB) treatment has improved in recent decades, such that approximately 85% of TB patients are effectively treated with a 6-month drug regimen consisting of isoniazid, rifampin, ethambutol, and pyrazinamide [1]. However, TB remains one of the top 10 mortality-associated diseases worldwide. Drug-resistant TB is one of the main factors contributing to this continued prevalence. Among the drug-resistant forms of TB, multidrug-resistant TB (MDR-TB) is resistant to isoniazid and rifampin [1]. Unlike the success rate of general TB treatment, the successful treatment of MDR-TB is dramatically lower (approximately 57% worldwide) and the MDR-TB treatment period is also longer (up to 24 month) and involves complicated dosing regimens related on a higher incidence of drug toxicity [1]. Thus, there is a need to explore appropriate treatments for MDR-TB.

Moxifloxacin (MOX), a respiratory quinolone, has been an important drug for treating a wide range of infections, especially pneumonia and TB [2]. Moxifloxacin is strongly recommended as a first-line drug for MDR-TB because of its high susceptibility [3]. Although several previous reports for optimal dose of MOX suggested 800 mg of MOX for MDR-TB patients, there were limitations to such a small dataset [4, 5], specific population groups [6, 7], and inclusion of other drug-resistant TB strains [8]. Therefore, an integrated study that emphasizes the optimal dose of MOX is needed to merge the various datasets and build an integrative model that explains the efficacy and toxicity of MOX [9].

In addition, a population lung lesion pharmacokinetics (PK) model has not been applied to MDR-TB patients. This model is a known predictor of drug response based on its description of systemic exposure and lung lesion distribution of MOX in TB patients [10]. QT interval prolongation, which can lead to arrhythmia, has been a major adverse reaction

Received 17 November 2021; editorial decision 21 December 2021; accepted 27 December 2021; published online 29 December 2021.

[a]M. J. J. and R. M. S. contributed equally to this manuscript.

Correspondence: Radojka M. Savic, PhD, Professor, Department of Bioengineering and Therapeutic Sciences, School of Pharmacy, University of California San Francisco, 1700 4th St., San Francisco, California 94158, USA (rada.savic@ucsf.edu).

Open Forum Infectious Diseases®2022

https://doi.org/10.1093/ofid/ofab660

associated with quinolones, including MOX [11, 12]; it is strongly associated with MOX exposure [13]. The QT prolongation prediction has not been found to reduce toxicity in MDR-TB patients.

The main purpose of this study was to develop a population PK model with a dataset consisting of MDR-TB patients of various ethnicities; it also aimed to conduct population PK modeling of lung lesion PK. Furthermore, a QT prolongation model was used to determine model-based efficacy and toxicity comparisons of MOX dosing regimens for MDR-TB.

METHODS

Study Population and Data Collection

Multidrug-resistant TB patients from 5 separate clinical trials were included in this study. The enrolled patients had been diagnosed with MDR-TB that exhibited resistance to isoniazid and rifampicin. Moxifloxacin (400 mg) was administered once daily for at least 2 weeks during the clinical trials. Patients were also administered a minimum of 2 additional MDR-TB medications. Blood samples were collected for analysis of MOX plasma concentrations by dense sampling after MOX administration. Plasma concentrations of MOX were determined using validated liquid chromatography-tandem mass spectrometry analysis [14–16].

Patient Consent Statement

All studies were approved by relevant national controlling bodies and ethical committees at the different sites and was done in accordance with Good Clinical Practice Guidelines and the principles of the Declaration of Helsinki (Table 1) (Study 1 [B-130191-001] by Institutional Review Board [IRB] at Seoul National University Bundang Hospital in Republic of Korea; Study 2 [ClinicalTrials.gov Identifier NCT0081646] by IRB at Pusan National University Hospital, Asan Medical Center and National Medical Center in Republic of Korea; Study 3 [ClinicalTrials.gov Identifier NCT01498419] by IRB at Karl Bremer Hospital, University of Cape Town Lung Institute Ltd, KwaZulu-Natal Research Institute for Tuberculosis and HIV, CHRU Themba Lethu Clinic, Klerksdorp Tshepong Hospital, Tembisa Hospital in South Africa and Ifakara Health Institute, Mbeya Medical Research Programme in Tanzania; Study 4 [ClinicalTrials.gov Identifier NCT02193776] by IRB at Tembisa Hospital, Klerksdorp Tshepong Hospital, TASK Applied Science, University of Cape Town Lung Institute Ltd, Tuberculosis & HIV Investigative Network of KwaZulu-Natal, CHRU Themba Lethu Clinic, Helen Joseph Hospital in South Africa and Ifakara Health Institute, Mbeya Medical Research Programme in Tanzania and Uganda Case Western Reserve University Research Collaboration in Uganda; Study 5 [ClinicalTrials.gov Identifier NCT02342886] by IRB at National Center for Tuberculosis and Lung Diseases in Georgia, Keny Medical Research Institute in Kenya, Pusat Perubatan Universiti Kebangsaan, Universiti Teknologi MARA, Institute of Respiratory Medicine in Malaysia, Philippine General Hospital, Vincent Balang, Lung Center of Philippines in Philippines; TASK, University of Cape Town Lung Institute, Setshaba Research Centre, Tembisa Hospital, CHRU Themba Lethu Clinic, Durban International Clinical Trials Unit, Klerksdorp Tshepong Hospital, Synexus SA, Madibeng Centre for Research, Tuberculosis & HIV Investigative Network of Kwazulu Natal, Aurum Institute, Aurum Institute: Rustenberg in South Africa, Ifakara Health Institute, Mbeya Medical Research Programme, Kilimanjaro National Institute for Medical Research in Tanzania, Uganda CWRU Research Collaboration in Uganda and Centre for Infectious Disease Research in Zambia). All patients provided written informed consent before the study.

Table 1. Baseline Characteristics of the Study Participants

Characteristic	Study 1	Study 2	Study 3	Study 4	Study 5	Total
Sex						
Male	4	10	14	39	6	73 (64.6%)
Female	5	5	8	16	6	40 (35.4%)
Ethnicity						
Black	-	-	12	48	8	68 (60.2%)
Mixed ethnic	-	-	10	6	3	19 (16.8%)
White and Asian	9	15	-	1	1	26 (23.0%)
HIV Status						
Negative	9	15	18	31	6	79 (69.9%)
Positive	-	-	5	24	6	35 (31.0%)
Age (years)	43 (34–89)	44 (23–59)	28 (20–56)	34 (18–69)	29 (20–61)	34 (18–89)
Weight (kg)	59 (47–67)	58 (50–84)	58 (40–82)	51 (35–71)	56 (43–75)	54 (35–84)
BMI (kg/m^2)	21.6 (17.6–23.2)	22.2 (17.3–29.4)	20.6 (16.4–29.7)	18.4 (12.2–27.1)	19.3 (16.9–27.8)	19.1 (12.2–29.7)
TB regimen	Pas, Cs, Kan, Pto, Z	Pas, Cs, Kan, Pto, Z	Pa, Z	J, Pa, Z	Pa, Z	-

Abbreviations: BMI, body mass index; Cs, cycloserine; HIV, human immunodeficiency virus; J, bedaquiline; Kan, kanamycin; Pa, proteomanid; Pas, *p*-aminosalicylic acid; Pto, prothionamide; TB, tuberculosis; Z, pyrazinamide.

NOTES: Study 1, B-130191-001; Study 2, NCT00816426; Study 3, NC002 (NCT01498419); Study 4, NC005 (NCT02193776); Study 5, NC006 (NCT02342886).

Population Pharmacokinetics Model Development

A nonlinear mixed-effects model (NONMEM 7.4; ICON, Dublin, Ireland) was used to develop the population PK model for MOX; a first-order conditional estimation with interaction option was used for the estimation method. Perl-speaks NONMEM (PsN) version 4.9.0 was used to assist the NONMEM in describing the graphical model evaluation; it was also used to perform automated covariate searching or bootstrap modeling [17]. Various compartment models, including one to multiple compartments, were explored as a structural model. A transit compartment model for the absorption phase [18], a flip-flop kinetics model for the absorption-elimination phase [19], and an allometric scaling model with body weight structural parameters [20] were also evaluated. An exponential relationship was used to explain interindividual variability (IIV). Furthermore, an additive, proportional, and combined model were tested to determine optimal residual variability (RV).

The selection of the model included both numerical criteria (eg, objective function value [OFV], shrinkage of IIV, and RV and precision of estimation values), diagnostic plots (eg, goodness-of-fit plot), and simulation-based diagnosis (eg, visual predictive check). The stepwise covariate modeling method was used to identify statistically significant parameter-covariate relationships, with $P < .05$ for forward selection and $P < .01$ for backward elimination. To figure out the final selected covariates, scientifical plausibility, clinical interest, and precision of parameter estimates were considered. The tested variables included sex, age, weight, body mass index (BMI), coadministration of TB drugs, and presence of human immunodeficiency virus (HIV). Nonparametric bootstrap modeling ($n = 500$) was performed as an internal model evaluation method.

Lung Lesion Distribution and QT Prolongation-Linked Population Pharmacokinetics Model

Lung lesion distribution and QT prolongation based on MOX PK were described using previously reported lung lesion distribution [10] and QT prolongation models [13]. Previous lung lesion distribution models of MOX indicated that lung lesion distribution is not connected to plasma concentration in a central compartment with intercompartmental rate constants (K_{pl}) and penetration partition coefficients (R_{pl}) for each lesion. Lung lesions were separated into 9 independent lesions, and an exponential IIV relationship was assumed for each lesion's partition coefficient. The RV was based on a proportional error model used in a previous report [10]. A link among QT prolongation, the baseline, and placebo-adjusted QT prolongation was established using the Fridericia heart rate correction method (*ΔΔQTcF*) and MOX concentration-QTc model by Florian et al [13, 21]. According to Florian et al [13], the plasma MOX concentration-QTc relationships was confirmed as linear model having slope and intercept, and they demonstrated those relationships through pooled analysis of 20 different studies. *ΔΔQTcF* was predicted using the linear equation: *ΔΔQTcF = Slope X Plasma concentration of MOX at time after dose + Intercept*. Similar to the PK-lung lesion distribution, an additive relationship was assumed for IIV and RV. Additional information concerning all parameters and equations is provided in Supplementary Methods 1.

Simulation for Probability Target Attainment

A simulation-based probability target attainment (PTA) was performed with efficacy and toxicity targets to optimize the MOX dosing regimen for MDR-TB patients. The ratio of the area under the concentration-time curve (AUC) of unbound drug to the minimum inhibitory concentration (MIC) is a well known parameter for predicting efficacy; the criteria are ≥100 for Gram-positive bacteria and ≥53 for *Mycobacterium tuberculosis* [7, 22–25]. Baseline MIC values for MOX were determined for isolated drug-resistant *M tuberculosis* from 194 patients in 2 clinical trials (NCT01498419 and NCT02342886). The MIC for MOX was determined by liquid culture by the mycobacteria growth indicator tube (MGIT) method that was standardized and pretrained across the sites [26, 27]. The peak (~35 μg/mL) and trough (~0.3–0.7 μg/mL) levels were used as concentration-based target levels for optimal MOX dose [4, 28]. QT prolongation toxicity was assessed using the change in *ΔΔQTcF* over 30 and 60 ms to determine high-risk criteria, on the basis of MOX induction case reports [29]. In accordance with the reports, 5 cases of moxifloxacin-induced Torsade de pointes have been reported in 2009, and this was the clue for setting over 60 ms as crucial criteria.

The PTA was calculated using the Monte Carlo simulation ($n = 1000$) with the final model to optimize MOX dosage. The MOX free fraction of area under the concentration curve (*f*AUC) was calculated using the simulation results from noncompartmental analysis with ncappc R package [30]. The unbound fraction of MOX was assumed to be 75% [8, 31], and simulation scenarios were developed in accordance with the World Health Organization (WHO) recommendation for MOX dose regimen, as well as the final selected covariates [3].

RESULTS

Demographics for Study Population

The demographic characteristics for MDR-TB patients are summarized in Table 1. In total, 113 adult patients were diagnosed with MDR-TB and their PK profiles were stratified according to HIV status (Figure 1). Patient plasma samples (1332) were collected from each clinical trial, along with covariate information concerning sex, age, weight, BMI, TB regimen, and HIV status. Covariate distributions were not skewed, and 16 samples (1.20%) below the limit of quantitation among total 1332 samples were excluded during the model development process.

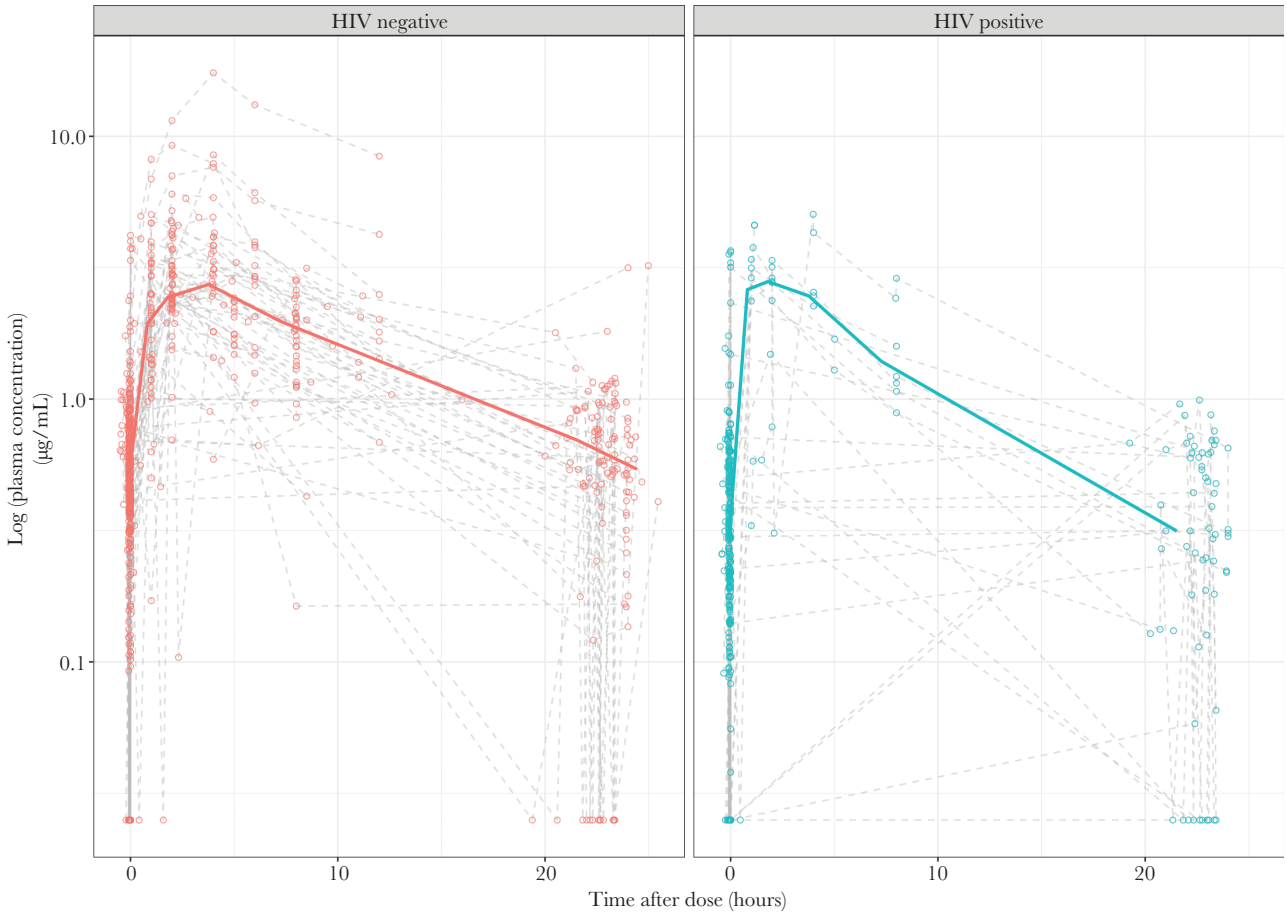

Figure 1. Plasma concentration versus time profile of moxifloxacin (MOX) after 400-mg dose administrations. (Left) Human immunodeficiency virus (HIV)-negative Multidrug-resistant tuberculosis (MDR-TB) patients. (Right) HIV-positive MDR-TB patients. A solid line and colored dots connected with a gray broken line represent the median and individual profiles, respectively.

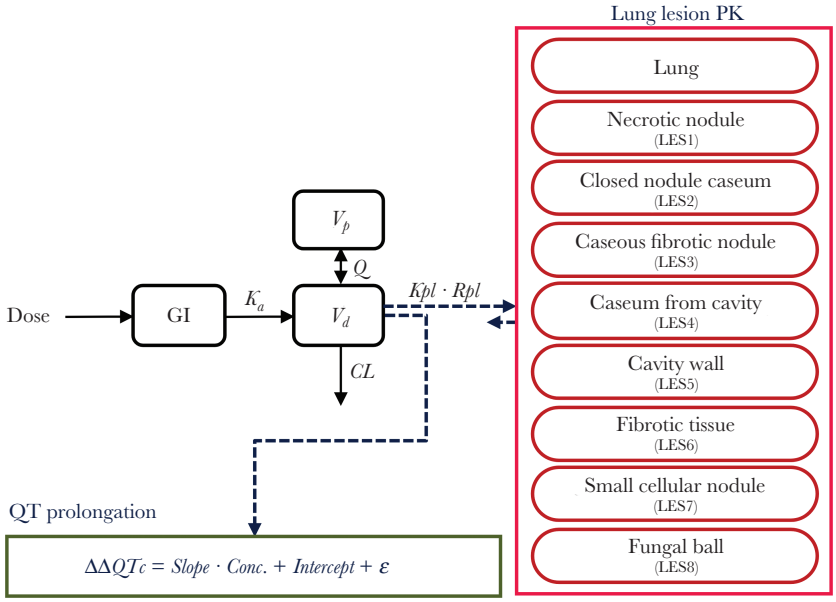

Figure 2. Final population pharmacokinetics model scheme for moxifloxacin.

Population Pharmacokinetics Model Development

A 2-compartment model with first-order absorption and elimination parameters was chosen as final structural model (Figure 2). The absorption model with lag time and transit compartment model were conducted; however, there was no significant improvement on OFV, visual predictive check (VPC), and the other diagnostic criteria. The other PK parameters related to absorption tended to be unstable with large relative standard errors. In addition, we observed unstable PK parameter estimations with a 3-compartment model. The implementation of IIV into intercompartmental clearance (Q) and volume of distribution for peripheral compartment (V_p) calculations was robust because of the high correlation observed when separate IIV values were used, in contrast to V_d and CL. Bioavailability (F) was fixed at a value of 1, based on a previous reported MOX bioavailability value (~86%) and because estimated values tended to be close to this value [32]. Human immunodeficiency virus status was selected as a covariate. The final estimated parameters and bootstrap results are reported in Table 2. The goodness-of-fit and visual predictive check plot for the final model are provided in Supplementary Figures S1 and S2.

Concentration-Based Target Attainment for Optimized Moxifloxacin Dosing Regimens for Multidrug-Resistant Tuberculosis

Recent WHO recommendations for MDR-TB treatment suggest a MOX dosing regimen of 800 mg per day [3]. We compared the simulated results between a dosage of 400 mg twice daily (BID) and 800 mg once daily (QD). The simulated PK profiles and AUC are shown in Figure 3A and B. The change in plasma concentration was greater for the 800-mg QD regimen than for the 400-mg BID regimen; however, the difference was not critical when considering differences in dose strength and frequency. The AUC was also not significantly different between the BID and QD regimens. The QD regimen was generally better than the BID regimen for MDR-TB patients, regardless of HIV status. This was demonstrated by the concentration-based target level for peak plasma concentration (C_{max}), plasma concentrations at 2 hours (C_2) and 6 hours (C_6) after dosing, and trough plasma concentrations (C_{trough}). However, the overall PTA did not surpass 50% for any regimen (Figure 4 and Supplementary Table S1).

Area Under the Concentration-Time Curve- and Minimum Inhibitory Concentration-Based Target Attainment Depending on Plasma and Lung Lesion Exposure

The baseline MIC distribution from 194 MDR-TB patients ranged from 0.03 to 0.5 µg/mL, with a high MIC frequency of 0.124 µg/mL (Supplementary Figure 3). Based on these results, the MIC range was set between 0.03 and 1 µg/mL to perform target attainment simulation. As the PK/pharmacodynamics target, *f*AUC/MIC values of ≥53 and ≥100 were calculated using concentrations captured from plasma and each lung lesion. The PTA was based on plasma concentrations (Table 3 and Figure 5). Human immunodeficiency virus-negative MDR-TB patients had better PTA values than HIV-positive patients in all ranges of MIC. However, all regimens within each group had inadequate PTA values at 1 µg/mL MIC. The PTA declined from over 0.25 µg/mL MIC to below 50% PTA at 1 µg/mL in all groups and regimens. No significant differences in PTA between BID and QD regimens were observed with respect to plasma concentration.

Time-versus-concentration profiles and *f*AUC/MIC values for each lung lesion are shown in Figure 6. The partition coefficient for MOX distribution between plasma and each lung lesion was >1; we observed higher exposure in all lung lesions. Therefore, the *f*AUC/MIC of each lesion had sufficient exposure in all subtypes at 0.5 µg/mL MIC. The effects of MOX are

Table 2. Final Estimated Parameters of Population Pharmacokinetics Models in MDR-TB Patients

	Population Estimates			Bootstrap	
Parameters	Value	RSE (%)	Shrinkage (%)	Median	5th–95th Percentile
K_a (hr^{-1})	1.07	20.2	-	1.05	0.775–1.664
V_d (L)	141	10.1	-	139	116–168
CL (L/h)	9.42	7.3	-	9.44	8.25–10.6
Q (L/h)	1.41	20.9	-	1.42	0.927–2.41
V_p (L)	886	24.4	-	862	523–1565
F (%)[a]	100	-	-	-	-
Coefficient of CL for HIV-positive[b]	0.327	33.3	-	0.321	0.131–0.548
Interindividual variability CV (%)					
IIV for V_d	55.2%	21.1	17.7	53.2%	29.9–82.5%
IIV for CL	67.9%	12.0	7.91	65.5%	49.5–85.1%
IIV for Q & V_p	373%	7.1	23.3	365%	243–518%
Residual variability (RV)					
Proportional error	24.3%	5.4	6.02	24.2%	20.4–28.9%

Abbreviations: CV, coefficient of variation; IIV, interindividual variability; MDR, multidrug resistant; RSE, relative standard error; TB, tuberculosis.

[a]Value was fixed.

[b]Equation for power coefficient was as follows: $CL_{HIV\ positive} = CL_{HIV\ negative} \cdot (1 + Coefficient)$.

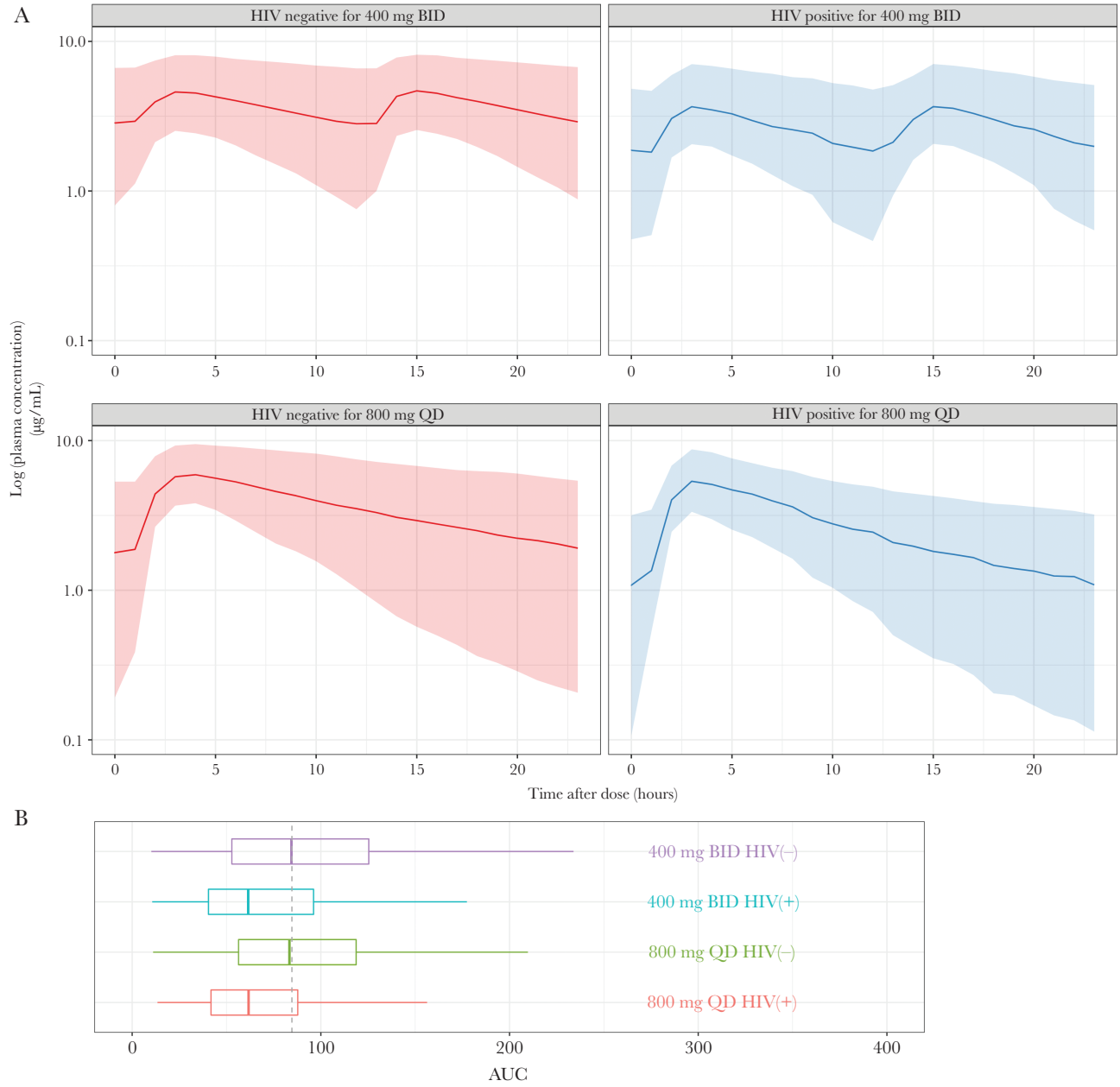

Figure 3. (A) Simulation pharmacokinetics profiles for moxifloxacin (MOX) at steady state after a twice-daily dose (BID) in the top panels and a once-daily dose (QD) in the bottom panels. The left panels represent human immunodeficiency virus (HIV)-negative samples; the right panels represent HIV-positive samples. (B) Area under the concentration curve (AUC) comparisons of MOX dosing regimens.

not expected because of sufficient exposure over 1.0 μg/mL. Moxifloxacin concentration should be maintained at a higher exposure level in HIV-negative patients. However, HIV status did not affect the target attainments for all subtypes of lung lesions.

QT Prolongation by Moxifloxacin Dosing Regimens in Multidrug-Resistant Tuberculosis Patients

The simulated *ΔΔQTcF* calculation using a model by Florian et al [13] and C_{max} for each MOX dosing regimen are described in Figure 7. The results of the linear regression and simulation studies indicated that the intercept for the 800-mg QD dosing regimens was approximately 2-fold higher than the 400-mg BID dose. These results indicated that *ΔΔQTcF* was higher at concentrations <5 μg/mL for the C_{max} group. Similar to the intercept results, the proportion of changes over 30 ms for *ΔΔQTcF* was approximately 2-fold greater in the 800-mg QD dosing regimen group (Table 4). Multidrug-resistant TB patients with HIV displayed protection because of their high *CL* value. Only 1% of MDR-TB patients without HIV were predicted to have a

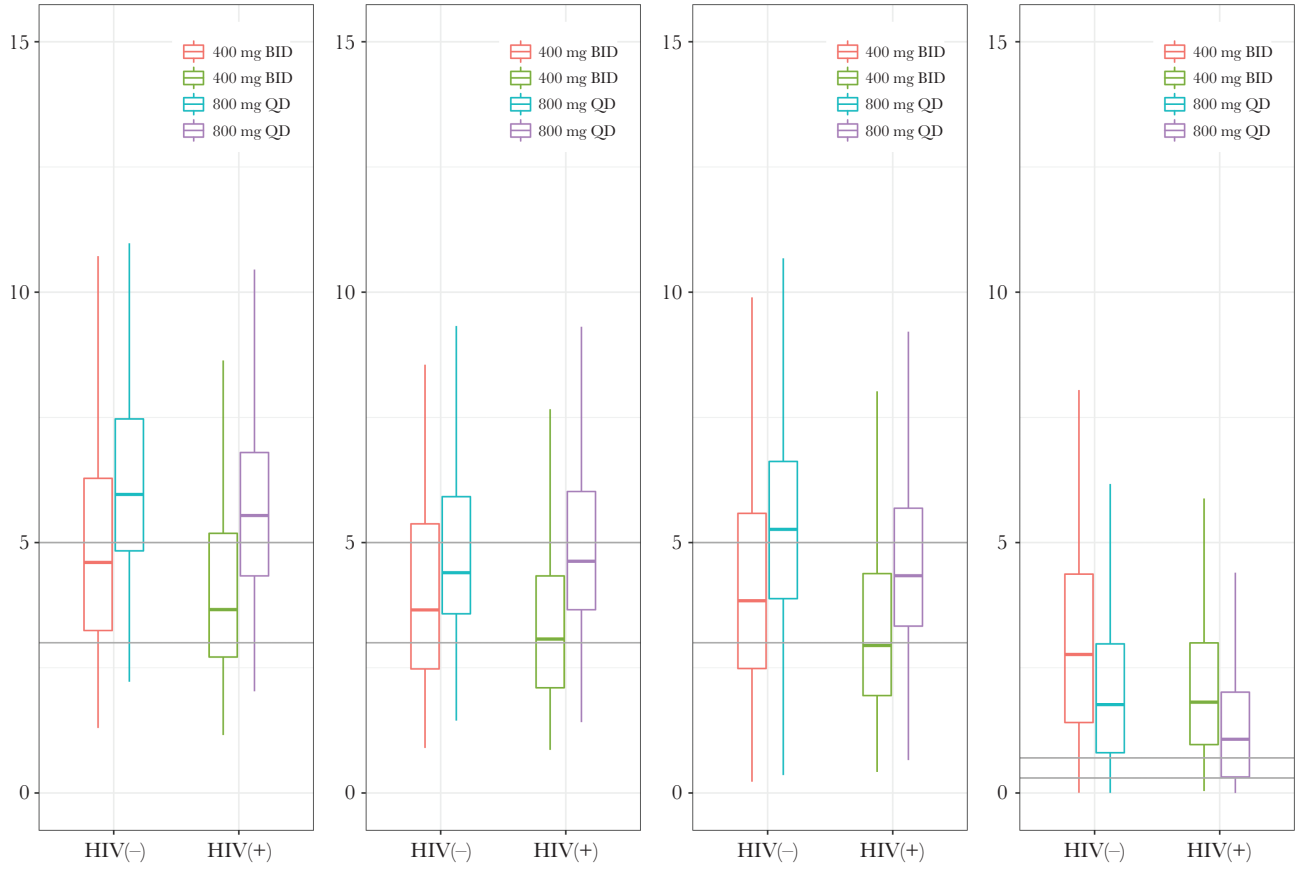

Figure 4. Concentration-based target attainment for (A) C_{max}; peak plasma concentrations, (B) C_2; plasma concentrations at 2 hours after dosing, (C) C_6; plasma concentrations at 6 hours after dosing, and (D) C_{trough}; trough plasma concentrations. The solid lines in (A), (B), and (C) represent a target range of ~3–5 µg/mL, and 0.3–0.7 µg/mL for (D). BID, twice-daily dose; HIV, human immunodeficiency virus; QD, once-daily dose.

Table 3. Probability %Target Attainment Accordingly Moxifloxacin Dosing Regimens

Target				
Schedule	BID Schedule		QD Schedule	
Status	HIV Negative	HIV Positive	HIV Negative	HIV Positive
MIC (µg/mL)	400 mg	400 mg	800 mg	800 mg
	*f*AUC/MIC Ratio ≥53			
0.03	100	100	100	100
0.06	100	100	100	100
0.125	100	98.0	100	99.5
0.25	98.0	86.1	99.5	84.6
0.5	93.0	48.8	90.0	44.3
1	59.7	11.4	62.2	5.97
	*f*AUC/MIC Ratio ≥100			
0.03	100	100	100	100
0.06	100	100	100	100
0.125	99.5	98.0	99.5	99.5
0.25	93.0	86.1	91.0	84.6
0.5	62.2	48.8	65.2	44.3
1	20.9	11.4	19.4	5.97

Abbreviations: BID, twice daily; *f*AUC, fraction of area under the concentration curve; HIV, human immunodeficiency virus; MIC, minimum inhibitory concentration; QD, once daily.

ΔΔQTcF of >60 ms with the 800-mg QD dosing regimen; this value was <1% for other patients and regimens.

DISCUSSION

We successfully developed a population PK model, which we merged with the lung lesion distribution and QT prolongation model, to determine model-based efficacy and toxicity of MOX in MDR-TB patients. The MOX 400-mg QD dosing regimen is used as the standard treatment for TB patients, whereas WHO guidelines and previous reports suggest advantages to using high MOX dosing regimens for MDR-TB patients [3, 4, 7]. Previous studies indicate that a 400-mg QD MOX dosing regimen is insufficient to treat MDR-TB patients, considering the concentration-based target and *f*AUC/MIC. We confirm here that a high MOX dosing regimen (800 mg QD or 400 mg BID) is sufficient for treatment of MDR-TB patients.

Based on previous MOX PK parameters, the *CL* of MOX is ~13.0 L/h (minimum value, ~11.6–15.0 L/h; maximum value, ~26–29 L/h) in healthy, non-TB patients [32–35]. An estimated 9.42 L/h (~8.25–10.6 L/h for the ~5th–95th percentiles) comprised a decrease of 27.5% in MDR-TB

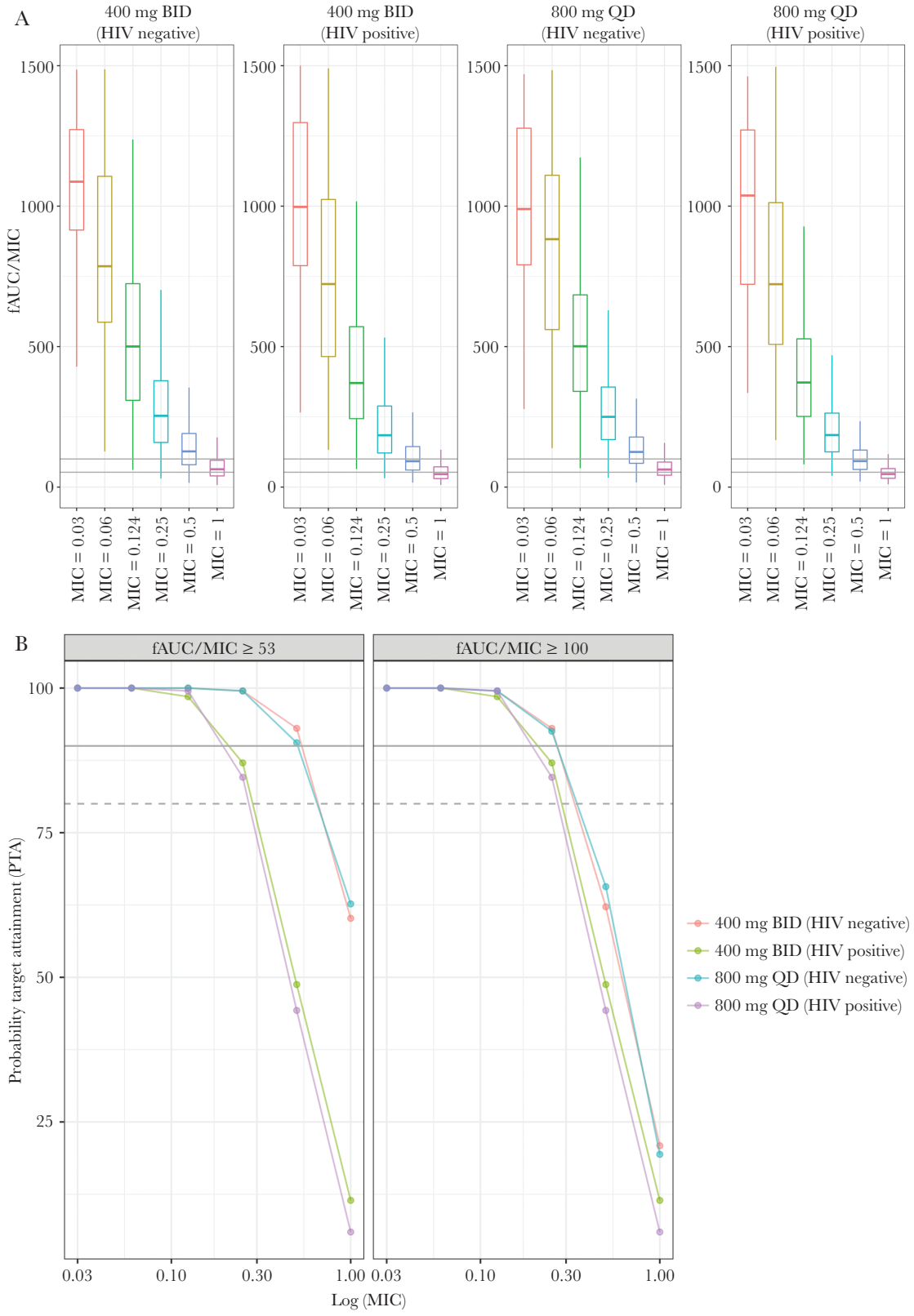

Figure 5. (A) Target attainment (fraction of area under the concentration curve [*f*AUC]/minimum inhibitory concentration [MIC] ≥53 for tuberculosis or ≥100 for Gram-positive bacteria) simulation for dosing regimens, and (B) the percentage of probability target attainment (PTA) on *f*AUC/MIC ≥53 and ≥100. The lower and upper solid lines in (A) represent *f*AUC/MIC ≥53 and ≥100. Solid and broken lines in (B) represent 90% and 80%, respectively. BID, twice-daily dose; HIV, human immunodeficiency virus; QD, once-daily dose.

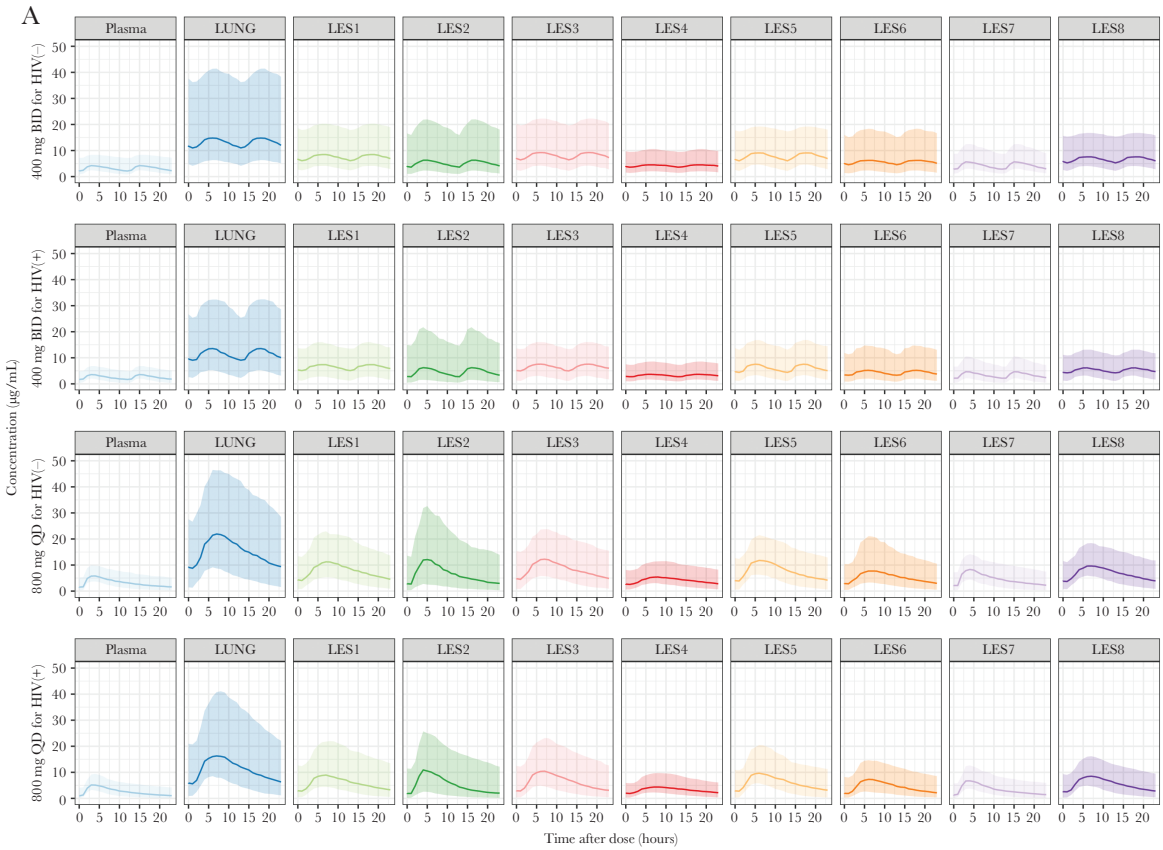

Figure 6. (A) Lung lesion concentration versus time profiles and (B) percent of probability target attainment (PTA) of fraction of area under the concentration curve (*f*AUC)/minimum inhibitory concentration (MIC) ≥53 and ≥100 for each lung lesion. The solid line and colored area in (A) represent the median and 90th percentile. The solid and dashed line in (B) represent an *f*AUC/MIC ≥53 and ≥100. BID, twice-daily dose; HIV, human immunodeficiency virus; LES1, necrotic nodule; LES2, closed nodule casein; LES3, caseous fibrotic nodule; LES4, caseum from cavity; LES5, cavity wall; LES6, fibrotic tissue; LES7, small cellular nodule; LES8, fungal ball; QD, once-daily dose.

patients. These differences were not statistically significant because of the large variability in MOX *CL*, which may have resulted from ethnicity factors that contributed to low *CL* values in Korean MDR-TB patients. Moxifloxacin is metabolized through glucuronide and sulphate conjugation by uridine diphosphate-glucuronosyltransferases (UGTs) and sulfotransferase, respectively [9]. UGT1A groups UGT1A1, UGT1A3, and UGT1A9 are responsible for MOX metabolism; they are highly polymorphic enzymes. UGT1A allele frequency is dependent on ethnicity and affects MOX PK in healthy volunteers. The pattern of UGT1A allele frequency in Korean populations is different from the patterns observed in both Caucasian and African American populations [36–38]. The dataset used for this study consisted of 20% Korean MDR-TB patients, which may have contributed to the low MOX *CL*. Further studies are needed to confirm the contribution of ethnicity.

Human immunodeficiency virus status was chosen as the final covariate, which resulted in a 32.7% increase in *CL* and 27.4% decrease in AUC. This phenomenon is explained by interactions with the drugs administered for HIV treatment. In a previous study by Naidoo et al [39], HIV treatment with efavirenz led to a drug interaction with MOX that increased *CL* by 42% and decreased AUC by 30%. Although information regarding the HIV dosing regimens was not included in our dataset, HIV status is an important covariate because the efavirenz-based HIV treatment regimen is widely used. With high MOX dosing regimens (400 mg BID and 800 mg QD), PTA and *f*AUC/MIC values of ≥53 and ≥100, respectively, were reached approximately 99% of the time with an MIC of 0.125 μg/mL, regardless of HIV status and dosing schedule. Patients with a maximum MIC (0.5 μg/mL) consisted of 7% of our dataset, and the 90th percentile of MIC was detected at 0.25 μg/mL. Moxifloxacin exposure in HIV-positive patients affected the PTA in the MIC range of 0.25 to 0.5 μg/mL. The AUC is expected to be lower in HIV-positive patients than in HIV-negative patients. The PTA dropped dramatically to ~50% at 0.5 μg/mL, whereas the PTA in HIV-negative patients remained approximately 90%. If the MIC was above 0.5 μg/mL, we would not expect an appropriate MOX effect for MDR-TB treatment for all regimens, as observed in our dataset.

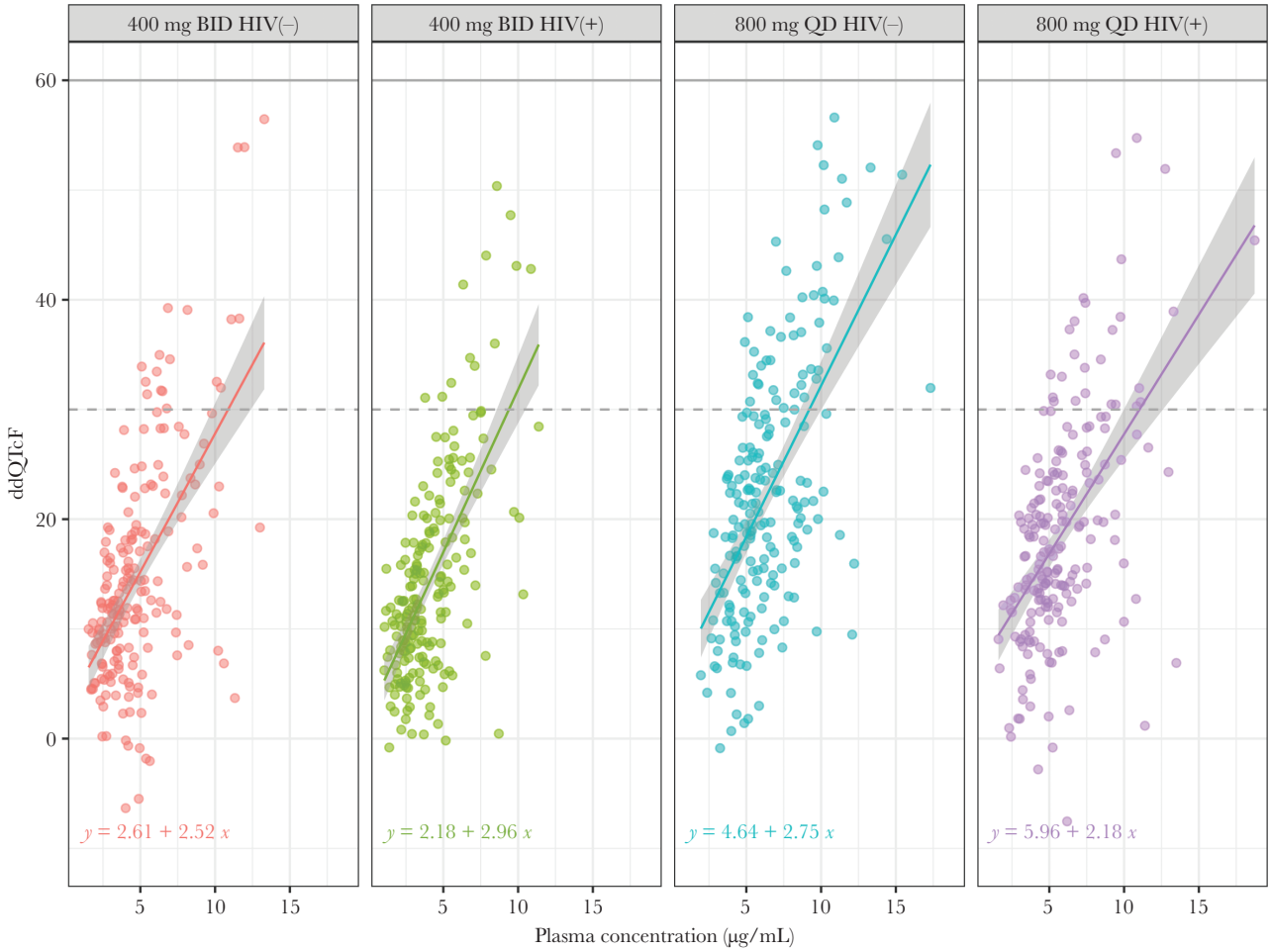

Figure 7. Relationship between ΔΔQTcF and C_{max} for moxifloxacin (MOX) dosing regimens. The solid and broken line represent a ΔΔQTcF ≥60 ms and ≥30 ms, respectively. BID, twice-daily dose; HIV, human immunodeficiency virus; QD, once-daily dose.

Moxifloxacin exposure covered all subtype lung lesions at 0.5 μg/mL MIC. This effect is not expected to be sufficient for samples of 1 μg/mL MIC, similar to the *f*AUC/MIC results in plasma. This is consistent with the finding by Sarathy et al [40] that a minimum 90% bactericidal concentration of MOX in casein was observed at a concentration of 2 μM (~5 μg/mL). The *f*AUC/MIC values of ≥53 and 100 were used as criteria, it must be considered that those kinds of scenarios came from the idea of Schentag et al [22, 23] studies what it originated from Gram-negative bacilli. Since the binding kinetics of fluoroquinolones should be different in mycobacteria and Gram-negative bacilli, the PTA results have to take into account of those matter of fact [41, 42].

QT prolongation is known to change in a MOX plasma concentration-dependent manner [11, 13, 29]. Therefore, a high MOX dosing regimen may carry a risk of QT prolongation. Crucial QT prolongation (≥ 60 ms) is not expected with the 400-mg BID dosing regimen in HIV-positive patients. This treatment regimen for HIV-positive patients is also considered safer than the 800-mg QD regimen because of the narrow fluctuation resulting from frequent and low dosing. Human immunodeficiency virus-positive patients have a high *CL*, and drug concentrations should be maintained at lower levels than in HIV-negative patients to reduce the QT prolongation risk.

Five different studies, which comprised MDR-TB patients with different ethnicities, were merged to discern the optimal MOX dosing regimens using the unified PK model with lung legion exposure and QT prolongation. Considering previous results that were restricted by sample size and patients characteristics, this approach could overcome the previous problems by merging the datasets. In addition, the first attempt to integrate

Table 4. Proportion (%) of 30 ms and 60 ms of ΔΔQTcF in MOX Dosing Regimen

Target	*ΔΔQTcF* ≥30 ms (%)		*ΔΔQTcF* ≥60 ms (%)	
Schedule	400 mg BID	800 mg QD	400 mg BID	800 mg QD
HIV negative	9.45	24.4	0.50	1.49
HIV positive	5.97	12.9	0.00	0.00

Abbreviations: BID, twice daily; HIV, human immunodeficiency virus; QD, once daily.

PK-lung legion-QT prolongation models supports our results because it gives us a perspective on the integrated considerations for efficacy and toxicity.

Limitations in this study included the assumption that the unbound fraction of MOX was identical across plasma samples and lung lesion subtypes. The MIC value was determined without using the results of Studies 1 and 2, which included mostly Korean MDR-TB patients. The application of these results to other populations must be carefully considered. Furthermore, the lung lesion and QT prolongation model was evaluated with previous estimated parameters through comparisons with previous reports; those results were determined by simulations, rather than observable data, because lung lesion and QT data were not collected for this study. Therefore, the parameters' re-estimation and recalculation for lung legion-QT prolongation models were not performed. The fact might be the limitation as well to expand the results to other population and conditions.

CONCLUSIONS

In conclusion, our results confirmed that a high MOX dosing regimen (800-mg daily dose) is effective for treatment of MDR-TB patients using simulation study with integrative model. In addition, a 400-mg twice-daily dose is expected to be safer than the 800-mg once-daily dose for reducing the risk of QT prolongation. Further clinical studies are needed to ensure the effectiveness and safety of MOX dosing regimens.

Acknowledgments

Financial support. This research was funded by Chungnam National University and the Institute of Information and Communications Technology Planning and Evaluation, using a grant funded by the government of the Republic of Korea (MSIT; No. 2020-0-01441, Artificial Intelligence Convergence Research Center, Chungnam National University).

Potential conflicts of interest. All authors: No reported conflicts of interest. All authors have submitted the ICMJE Form for Disclosure of Potential Conflicts of Interest.

References

1. World Health Organization (WHO). Global tuberculosis report 2020. Geneva: World Health Organization (WHO); **2020**.
2. Grossman RF, Hsueh PR, Gillespie SH, Blasi F. Community-acquired pneumonia and tuberculosis: differential diagnosis and the use of fluoroquinolones. Int J Infect Dis **2014**; 18:14–21.
3. World Health Organization (WHO). WHO consolidated guidelines on tuberculosis treatment. Geneva: World Health Organization (WHO); **2019**.
4. Chang MJ, Jin B, Chae JW, et al. Population pharmacokinetics of moxifloxacin, cycloserine, p-aminosalicylic acid and kanamycin for the treatment of multidrug-resistant tuberculosis. Int J Antimicrob Agents **2017**; 49:677–87.
5. Peloquin CA, Hadad DJ, Molino LPD, et al. Population pharmacokinetics of levofloxacin, gatifloxacin, and moxifloxacin in adults with pulmonary tuberculosis. Antimicrob Agents Chemother **2008**; 52:852–7.
6. Willmann S, Frei M, Sutter G, et al. Application of physiologically-based and population pharmacokinetic modeling for dose finding and confirmation during the pediatric development of moxifloxacin. CPT Pharmacometrics Syst Pharmacol **2019**; 8:654–63.
7. Zvada SP, Denti P, Sirgel FA, et al. Moxifloxacin population pharmacokinetics and model-based comparison of efficacy between moxifloxacin and ofloxacin in African patients. Antimicrob Agents Chemother **2014**; 58:503–10.
8. Pranger AD, Van Altena R, Aarnoutse RE, et al. Evaluation of moxifloxacin for the treatment of tuberculosis: 3 years of experience. Eur Respir J **2011**; 38:888–94.
9. Naidoo A, Naidoo K, McIlleron H, Essack S, et al. A review of moxifloxacin for the treatment of drug-susceptible tuberculosis. J Clin Pharmacol **2017**; 57:1369–86.
10. Strydom N, Gupta SV, Fox WS, et al. Tuberculosis drugs' distribution and emergence of resistance in patient's lung lesions: a mechanistic model and tool for regimen and dose optimization. PLoS Med **2019**; 16:1–26.
11. Bertino JJ, Fish D. The safety profile of the fluoroquinolones. Clin Ther **2000**; 22:798–817; discussion 797.
12. Altin T, Ozcan O, Turhan S, et al. Torsade de pointes associated with moxifloxacin: a rare but potentially fatal adverse event. Can J Cardiol **2007**; 23:907–8.
13. Florian JA, Tornøe CW, Brundage R, Parekh A, et al. Population pharmacokinetic and concentration-QTc models for moxifloxacin: pooled analysis of 20 thorough QT studies. J Clin Pharmacol **2011**; 51:1152–62.
14. Kjellsson MC, Via LE, Goh A, et al. Pharmacokinetic evaluation of the penetration of antituberculosis agents in rabbit pulmonary lesions. Antimicrob Agents Chemother **2012**; 56:446–57.
15. Han M, Jun SH, Lee JH, Park KU, Song J, et al. Method for simultaneous analysis of nine second-line anti-tuberculosis drugs using UPLC-MS/MS. J Antimicrob Chemother **2013**; 68:2066–73.
16. Conde MB, Mello FCQ, Duarte RS, et al. A phase 2 randomized trial of a rifapentine plus moxifloxacin-based regimen for treatment of pulmonary tuberculosis. PLoS One **2016**; 11:1–13.
17. Lindbom L, Pihlgren P, Jonsson EN. PsN-Toolkit--a collection of computer intensive statistical methods for non-linear mixed effect modeling using NONMEM. Comput Methods Programs Biomed **2005**; 79:241–57.
18. Savic RM, Jonker DM, Kerbusch T, Karlsson MO. Implementation of a transit compartment model for describing drug absorption in pharmacokinetic studies. J Pharmacokinet Pharmacodyn **2007**; 34:711–26.
19. Yáñez JA, Remsberg CM, Sayre CL, Forrest ML, Davies NM. Flip-flop pharmacokinetics—delivering a reversal of disposition: Challenges and opportunities during drug development. Ther Deliv **2011**; 2:643–72.
20. Back HM, Lee JB, Han N, et al. Application of size and maturation functions to population pharmacokinetic modeling of pediatric patients. Pharmaceutics **2019**; 11:259–71.
21. Fridericia LS. Die Systolendauer im Elektrokardiogramm bei normalen Menschen und bei Herzkranken. Acta Med Scand **1920**; 53:469–86.
22. Schentag JJ, Meagher AK, Forrest A. Fluoroquinolone AUIC break points and the link to bacterial killing rates. Part 1: in vitro and animal models. Ann Pharmacother **2003**; 37:1287–98.
23. Schentag JJ, Meagher AK, Forrest A. Fluoroquinolone AUIC break points and the link to bacterial killing rates. Part 2: human trials. Ann Pharmacother **2003**; 37:1478–88.
24. Shandil RK, Jayaram R, Kaur P, et al. Moxifloxacin, ofloxacin, sparfloxacin, and ciprofloxacin against *Mycobacterium tuberculosis*: evaluation of in vitro and pharmacodynamic indices that best predict in vivo efficacy. Antimicrob Agents Chemother **2007**; 51:576–82.
25. Gumbo T, Louie A, Deziel MR, Parsons LM, Salfinger M, et al. Selection of a moxifloxacin dose that suppresses drug resistance in *Mycobacterium tuberculosis*, by use of an in vitro pharmacodynamic infection model and mathematical modeling. J Infect Dis **2004**; 190:1642–51.
26. Dawson R, Diacon AH, Everitt D, et al. Efficiency and safety of the combination of moxifloxacin, pretomanid (PA-824), and pyrazinamide during the first 8 weeks of antituberculosis treatment: a phase 2b, open-label, partly randomised trial in patients with drug-susceptible or drug-resistant pul. Lancet **2015**; 385:1738–47.
27. Diacon AH, Maritz JS, Venter A, et al. Time to detection of the growth of *Mycobacterium tuberculosis* in MGIT 960 for determining the early bactericidal activity of antituberculosis agents. Eur J Clin Microbiol Infect Dis **2010**; 29:1561–5.
28. Alsultan A, Peloquin CA. Therapeutic drug monitoring in the treatment of tuberculosis: An update. Drugs **2014**; 74:839–54.
29. Khan F, Ismail M, Khan Q, Ali Z. Moxifloxacin-induced QT interval prolongation and torsades de pointes: a narrative review. Expert Opin Drug Saf **2018**; 17:1029–39.
30. Acharya C, Hooker AC, Türkyılmaz GY, Jönsson S, et al. A diagnostic tool for population models using non-compartmental analysis: the ncappc package for R. Comput Methods Programs Biomed **2016**; 127:83–93.
31. Dorn C, Nowak H, Weidemann C, et al. Decreased protein binding of moxifloxacin in patients with sepsis. GMS Infect Dis **2017**; 5:1–6.
32. Stass H, Kubitza D. Pharmacokinetics and elimination of moxifloxacin after oral and intravenous administration in man. J Antimicrob Chemother **1999**; 43:83–90.
33. Stass H, Dalhoff A, Kubitza D, Schühly U. Pharmacokinetics, safety, and tolerability of ascending single doses of moxifloxacin, a new 8-methoxy

quinolone, administered to healthy subjects. Antimicrob Agents Chemother **1998**; 42:2060–5.
34. Öbrink-Hansen K, Hardlei TF, Brock B, et al. Moxifloxacin pharmacokinetic profile and efficacy evaluation in empiric treatment of community-acquired pneumonia. Antimicrob Agents Chemother **2015**; 59:2398–404.
35. Dekkers BGJ, Bolhuis MS, Beek L, et al. Reduced moxifloxacin exposure in patients with tuberculosis and diabetes. Eur Respir J **2019**; 54:2–5.
36. Hasunuma T, Tohkin M, Kaniwa N, et al. Absence of ethnic differences in the pharmacokinetics of moxifloxacin, simvastatin, and meloxicam among three East Asian populations and Caucasians. Br J Clin Pharmacol **2016**; 81:1078–90.
37. Shimoyama S. Pharmacogenetics of irinotecan: an ethnicity-based prediction of irinotecan adverse events. World J Gastrointest Surg **2010**; 2:14.
38. Naidoo A, Ramsuran V, Chirehwa M, et al. Effect of genetic variation in UGT1A and ABCB1 on moxifloxacin pharmacokinetics in South African patients with tuberculosis. Pharmacogenomics **2018**; 19:17–29.
39. Naidoo A, Chirehwa M, McIlleron H, et al. Effect of rifampicin and efavirenz on moxifloxacin concentrations when co-administered in patients with drug-susceptible TB. J Antimicrob Chemother **2017**; 72:1441–9.
40. Sarathy JP, Via LE, Weiner D, et al. Extreme drug tolerance of *Mycobacterium tuberculosis* in caseum. Antimicrob Agents Chemother **2018**; 62:1–11.
41. Drlica K, Malik M, Kerns RJ, Zhao X. Quinolone-mediated bacterial death. Antimicrob Agents Chemother **2008**; 52:385–92.
42. Drlica K, Hiasa H, Kerns R, Malik M, et al. Quinolones: action and resistance updated. Curr Top Med Chem **2009**; 9:981–98.